THE JOURNAL OF BIOLOGICAL CHEMISTRY VOL. 281, NO. 20, pp. 14256–14262, May 19, 2006

Modular Structure of the Receptor Binding Proteins of *Lactococcus lactis* Phages

*THE RBP STRUCTURE OF THE TEMPERATE PHAGE TP901-1**

Received for publication, January 23, 2006, and in revised form, March 17, 2006 Published, JBC Papers in Press, March 20, 2006, DOI 10.1074/jbc.M600666200

Silvia Spinelli[‡1], Valérie Campanacci[‡1], Stéphanie Blangy[‡], Sylvain Moineau[§¶‖], Mariella Tegoni[‡], and Christian Cambillau[‡2]

From [‡]Architecture et Fonction des Macromolécules Biologiques, UMR 6098 CNRS and Universités d'Aix-Marseille I and II, Campus de Luminy, Case 932, 13288 Marseille Cedex 09, France and the [§]Groupe de Recherche en Écologie Buccale, Faculté de Médecine Dentaire, the [¶]Félix d'Hérelle Reference Center for Bacterial Viruses, and the [‖]Département de Biochimie et de Microbiologie, Faculté des Sciences et de Génie, Université Laval, Québec City, Québec G1K 7P4, Canada

***Lactococcus lactis* is a Gram-positive bacterium widely used by the dairy industry. Several industrial *L. lactis* strains are sensitive to various distinct bacteriophages. Most of them belong to the *Siphoviridae* family and comprise several species, among which the 936 and P335 are prominent. Members of these two phage species recognize their hosts through the interaction of their receptor-binding protein (RBP) with external cell wall saccharidices of the host, the "receptors." We report here the 1.65 Å resolution crystal structure of the RBP from phage TP901-1, a member of the P335 species. This RBP of 163 amino acids is a homotrimer comprising three domains: a helical N terminus, an interlaced β-prism, and a β-barrel, the head domain (residues 64–163), which binds a glycerol molecule. Fluorescence quenching experiments indicated that the RBP exhibits high affinity for glycerol, muramyl-dipeptide, and other saccharides in solution. The structural comparison of this RBP with that of lactococcal phage p2 RBP, a member of the 936 species (Spinelli, S., Desmyter, A., Verrips, C. T., de Haard, J. W., Moineau, S., and Cambillau, C. (2006) *Nat. Struct. Mol. Biol.* 13, 85–89) suggests a large extent of modularity in RBPs of lactococcal phages.**

Phages of *Lactococcus lactis* are a major problem in industrial milk fermentation, because they are ubiquitous within their process environments as well as within pasteurized milk (1). They belong to several different species of the *Siphoviridae* family (small isometric capsid and long noncontractile tail), among which the genetically distinct species 936, P335, and c2 are the three prominent (2–7).

The first steps of phage infection require interactions between the phage receptor-binding proteins (RBPs)[3] (8, 9) and the receptors at the host cell surface. These mediating RBPs are located at the distal structure of their long tail (150–200 nm). Lactococcal phages from species 936 or P335 bind to carbohydrate receptors at the surface of the cell wall, the exact nature of them being still unknown (10–15). A better understanding at a molecular level of this recognition mechanism would increase the possibility of designing novel tools to inactivate the RBPs, thereby preventing phage infection.

In this context, solving the structure of lactococcal phage RBPs is a significant step in understanding the phage-host interactions. To this end, we have previously determined the first crystal structure of a RBP from a lactococcal phage, namely from the lytic phage p2 (936 species) (16). This RBP is formed of three monomers related by a 3-fold noncrystallographic axis, each assembling three domains, from N to C terminus: the shoulders, the interlaced neck, and the heads. We have shown that this last domain harbors the putative saccharide-binding site, which can be blocked by a llama immunoglobulin VH domain of camelid antibody heavy chain (9, 16, 17). We recently showed that the binding of a glycerol molecule to the head domain led to the identification of the residues of the saccharide-binding site (15).

The lactococcal temperate phage TP901-1 belongs to the P335 species. It has a genome size of 37,667 bp with 56 open reading frames (ORFs) (18). Phage TP901-1 has a long noncontractile tail with a distal baseplate (19). Recently, one of its ORFs (ORF49 or BppL) has been identified as being the phage RBP (11, 20). The mechanism of assembly of the baseplate of phage TP901-1 was also recently deciphered, indicating that BppL forms the lower baseplate and is the last component to be assembled (19). In the present study, we have solved the second RBP structure of a lactococcal phage, namely the RBP (BppL) of TP901-1 (20), using molecular replacement with the head domain of p2 RBP as a starting model. As with the latter, the RBP of phage TP901-1 harbors a glycerol molecule located in a saccharide binding site of the C-terminal domain. Tryptophan fluorescence quenching experiments performed with a F145W mutant indicated that, in solution, the RBP of TP901-1 binds strongly to glycerol, phosphoglycerol, *N*-acetylmuramic acid, and muramyl-dipeptide.

EXPERIMENTAL PROCEDURES

Native RBP Production and Crystallization—The ORF49 (RBP) of phage TP901-1 was cloned in the Gateway™ pDEST17 vector (21) according to standard procedures as described previously. A tobacco etch virus protease cleavage site was inserted between the ATTB1 and the gene of interest. The resulting vector was transformed in *Escherichia coli* Rosetta-pLysS strains. Cells were grown at 28 °C in terrific broth medium in agitated flasks (4 × 750 ml) until the OD reached 0.5 and then induced with isopropyl 1-thio-β-D-galactopyranoside (0.5 mM). After cell centrifugation, lysis was performed in 150 ml of lysis solution (50 mM Tris, 150 mM NaCl, 10 mM imidazole, pH 8.0, 0.25 mg/ml lysozyme, 1 mM PMSF). Purification was performed in two steps, a Ni^{2+}-NTA column, followed by gel filtration (HiLoad S200) on a GE Δkta fast protein liquid chromatograph. The protein was concentrated

* This work was supported by the Genopole of Marseille-Nice and by the Natural Sciences and Engineering Research Council of Canada. The costs of publication of this article were defrayed in part by the payment of page charges. This article must therefore be hereby marked "*advertisement*" in accordance with 18 U.S.C. Section 1734 solely to indicate this fact.

The atomic coordinates and structure factors (code 2F0C) have been deposited in the Protein Data Bank, Research Collaboratory for Structural Bioinformatics, Rutgers University, New Brunswick, NJ (http://www.rcsb.org/).

[1] These authors contributed equally to this work.

[2] To whom correspondence should be addressed. Fax: 33-491-266-720; E-mail: cambillau@afmb.univ-mrs.fr.

[3] The abbreviations used are: RBP, receptor binding protein; ORF, open reading frame; r.m.s., root mean square; EM, electron microscopy; BppL, baseplate protein lower.

to 5.6 mg/ml (2.5 mg total) and subjected to crystallization screening with a Cartesian nanodrop-dispensing robot (22). Crystals were obtained at 20 °C by mixing 300 nl of protein (5 mg/ml in 1.8 mM KH_2PO_4, 10.1 mM NaH_2PO_4, 2.7 mM KCl, 137 mM NaCl, pH 7.2) with 100 nl of precipitant solution containing 2 M ammonium sulfate, 0.2 M sodium/potassium tartrate and 0.1 M sodium citrate (pH 6.5). Crystals appeared after 1 week. Crystal were fished using a nylon loop and frozen in a synthetic solution of crystallization medium containing 40% glycerol as cryoprotectant. Crystals belong to the P $2_12_12_1$ space group with cell dimensions a = 72.5 Å, b = 78.7 Å, and c = 81.7 Å. They contain a biological trimer in the asymmetric unit (V_m = 2.09 Å^3/Da (23); 40.6% solvent).

F145W BppL Production—The single amino acid mutation was generated using the method developed by Zheng *et al.* (24) and derived from the QuikChange™ site-directed mutagenesis protocol (Stratagene). Briefly, the pDEST17/BppL vector was entirely amplified by the Platinum® Pfx DNA polymerase (Invitrogen) using two partial overlapping mutated primers; the Phe^{145} codon was mutated to encode Trp (in boldface type) using the primers Phe145Trp-F (5′-GTATGTCAGTGG**TGG**GGTCCAACTGCGAGCAGTGGTACTCCTCG-3′) and Phe145Trp-R (5′-CGCAGTTGGACC**CCA**CCACTGACATACTCCACTTGATGG-3′). The PCR amplification products were evaluated by agarose gel electrophoresis and were further treated with restriction enzyme DpnI (Fermentas) to eliminate the native plasmid. An aliquot of 1 μl was transformed into DH1OB T1R chemocompetent cells and spread on an LB plate containing 100 μg/ml ampicillin. Expression and purification were performed as for the native protein.

Fluorescence Quenching Experiments—Fluorescence experiments were carried out on a Varian Eclipse spectrofluorimeter using a quartz cuvette in a right angle configuration; light path was 0.4 and 1 cm for the excitation and emission, respectively. The interaction of RBP with saccharides was monitored by recording the quenching of the intrinsic protein fluorescence upon the addition of ligand aliquots. Excitation wavelength was 290 nm, and emission spectra were recorded in the range 320–380 nm. The excitation slit was 5 nm, whereas the emission slit was 20 nm for a protein concentration of 1 μM. A moving average smoothing procedure was applied, with a window of 3 nm. Titrations were carried out at room temperature with 1 μM protein in 10 mM phosphate buffer Na/Na_2, 50 mM NaCl, pH 7.5. The fluorescence intensities at the maximum of emission (340 nm) for different concentrations of quencher were corrected for the buffer contribution before plotting and further analysis. The affinity was estimated by plotting the decrease of fluorescence intensity at the emission maximum as $(100 - (I_i - I_{min})/(I_0 - I_{min}) \times 100)$ against the quencher concentration; I_0 is the maximum of fluorescence intensity of the protein alone, I_i is the fluorescence intensity after the i addition of quencher, I_{min} is the fluorescence intensity at saturating concentration of quencher. The K_d values were estimated using Prism 3.02 (GraphPad Software, Inc.), by nonlinear regression for a single binding site with the equation $Y = B_{max} \times X/(K_d + X)$, where B_{max} is the maximal binding and K_d is the concentration of ligand required to reach half-maximal binding.

Crystallographic Study of TP901-1 RBP—The 1.65 Å data set was collected at beam line ID14–3 (European Synchrotron Radiation Facility, Grenoble, France). A total of 400 images (0.5° rotation) were collected on an ADSC Quantum 4 detector. Data were integrated and reduced using MOSFLM and SCALA (25). Molecular replacement was performed with AMoRe (26) using the phage p2 RBP head trimer as search model (Protein Data Bank number 1BSD; residues 162–264). The correlation coefficient and R-factor at 3.5 Å were 0.22 and 0.517, respectively, whereas those for the next solutions were lower than 14.5 and larger than 0.541, respectively. Refinement was performed with REFMAC5 (27) alternated with rebuilding using Turbo-Frodo (28). After rebuilding and refining the head domain, improved statistics and maps were obtained (R_{free} = 0.39, R = 0.34). At this stage, a better electron density map made it possible to trace the rest of the molecule (residues 16–70). Due to deviations from a true 3-fold symmetry, the first 20 residues had to be built independently in each of the monomer. The first 15 residues in sequence are not visible in the electron density map, due to proteolysis and disorder. 95.7% of the residues are found in the PROCHECK (29) most favorable region, and 4.3% are found in the additional allowed region. Statistics of data collection and model refinement are presented in Table 1.

TABLE 1
Data collection and refinement statistics

Parameters	Values
Data collection	
Percentage of data >1σ overall (last shell)	100 (100)
Overall I/σ (I) (last shell)	7.5 (2.6)
Resolution Limits (Å) overall (last shell)	40.0-1.65 (1.74-1.65)
R_{merge} (%) overall (last shell)	7.8 (29.6)
Data refinement	
Protein/glycerol/solvent atoms	3251/18/715
Resolution limits (Å) overall (last shell)	31.8-1.65 (1.65-1.69)
R/R_{free} value (%) overall (last shell)	0.156/0.19 (0.163/0.225)
r.m.s. deviation on bonds (Å)/angles (degrees)	0.010/1.3
Mean B factor (Å^2)	
Protein	12.5
Glycerol, monomer A/B/C	29/17/23
Water	28.5

RESULTS

Overall RBP Structure—The RBP of phage TP901-1 is 163 amino acids long, which is significantly shorter than the RBP of the lactococcal phage p2 (264 residues). However, its C-terminal domain (residues 64–163) appears to be of the same length as the head domain of p2 RBP (residues 162–264, Fig. 1*A*), and it shares 28% identity, suggesting that their folds should be similar. In contrast, the N-terminal domain of the RBP of TP901-1 comprises only 63 residues as compared with 161 amino acids of p2 RBP, and no sequence similarity can be detected between them (Fig. 1*A*). Finally, it should be noted that these two phages (TP901-1 and p2) do not infect the same *L. lactis* strains, and thus, their respective RBPs have their own specificity.

The RBP of phage TP901-1 is formed of three chains associated in a homotrimer of overall dimensions 90 × 45 × 45 Å (Fig. 1*B*). The three monomers are related by a noncrystallographic 3-fold axis coincident with the long axis of the trimer (*vertical* in Fig. 1, *B* and *D*). The first 15 (B monomer) or 16 (A and C monomers) amino acids of the 163-residue peptidic chain are not visible in the electron density map. SDS gels reveal, however, the presence of both intact and cleaved forms of RBP monomers, with a mass difference of ~5000 Da. This value is compatible with a segment of 27 residues comprising from the expression vector the His_6, the ATTB1, and the tobacco etch virus protease cleavage site plus the 15/16 first residues of the native RBP sequence, with theoretical masses of 5007 and 5133 Da. The SDS gels and the fact that RBP can be purified on Ni^{2+}-NTA columns converge to indicate that several forms of trimers may coexist containing one or two cleaved chains associated with two or one intact chain. The N termini of these intact chains are disordered in the crystal, probably due to the lack of intertrimer or packing interactions. Crystal packing examination confirms that the missing residues should point out in the bulk solvent and do not interact with symmetry-related RBP molecules.

The RBP trimer is organized into three regions: an N-terminal parallel three-helix bundle, an interlaced β-prism (also named the β-helix),

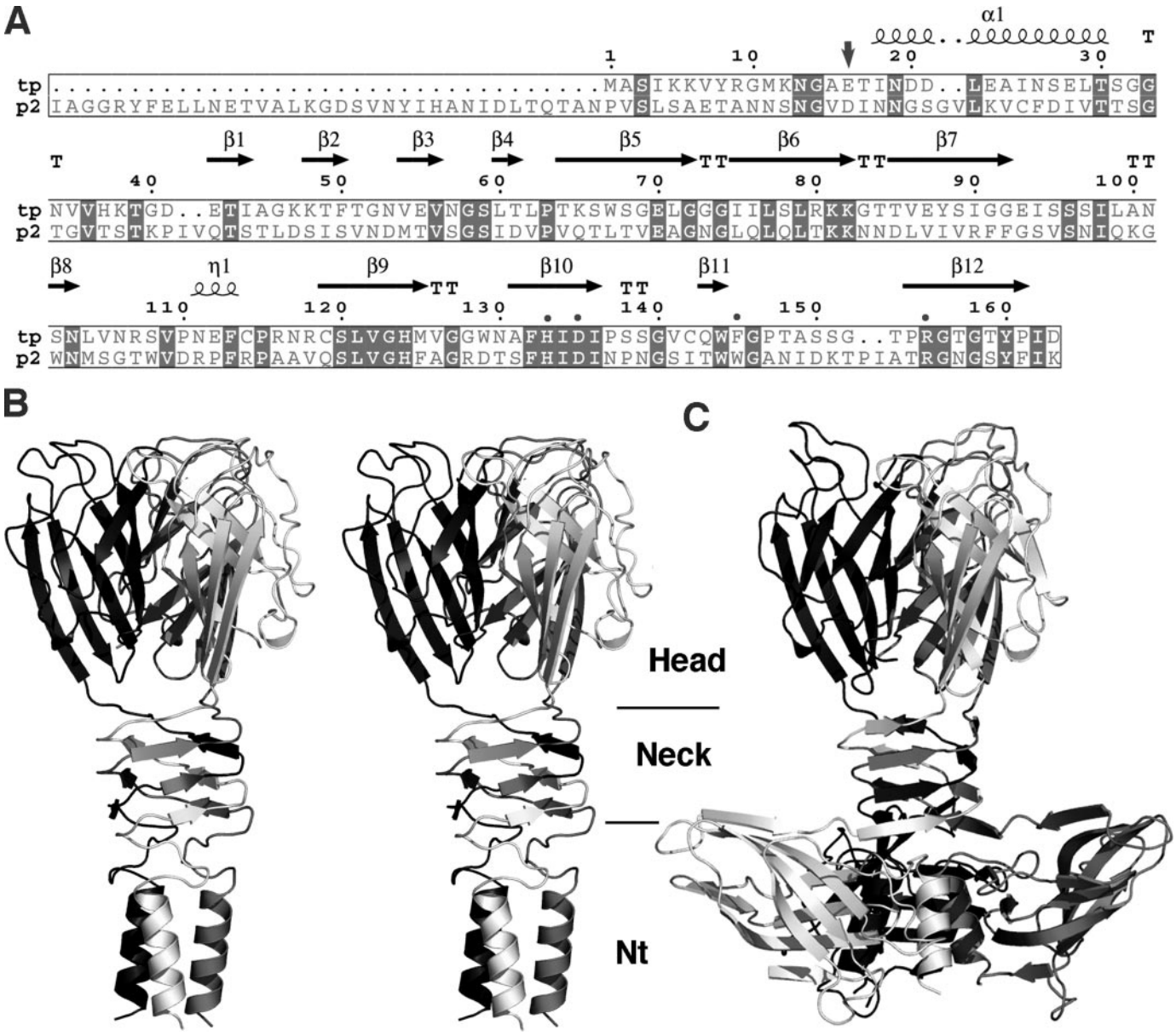

FIGURE 1. Compared sequence (*A*) and structure (*B*) of the RBPs from lactococcal phages TP901-1 and p2. *A*, sequence alignment and secondary structure are displayed for phages TP901-1 (*tp*) and p2. The *arrow* indicates where the chain starts in the electron density map. The *filled circles* identify the residues involved in glycerol binding in both RBPs (alignment made by MULTALIN (available on the World Wide Web at prodes.toulouse.inra.fr/multalin/multalin.html)). *B*, ribbon stereo view of the TP901-1 RBP trimer; *C*, compared with the p2 RBP trimer. Both RBPs are at the same scale and colored *black*, *dark gray*, and *gray*. The three domains, N-terminal (or shoulders in p2), neck and head have been labeled *Nt*, *Neck*, and *Head*, respectively (views made with Pymol (available on the World Wide Web at www.pymol.org)).

and a C-terminal six-stranded β-barrel (Fig. 1*B*). This trimeric arrangement is frequently observed in fibers or RBPs from mammalian viruses (30, 31) as well as from bacteriophages (16, 32). The three polypeptidic chains of the trimer display close structures (r.m.s. deviation values of 0.66–0.82 Å for Cα atoms). The head domains are quasi-identical, within the coordinate errors, with 0.16–0.22 Å r.m.s. deviation. The largest deviations are observed at the three N-terminal ends of RBP.

Indeed, the RBP trimer interactions involve a large percentage of buried surface area (42%; 4208 of 10,070 Å^2), due in a large part to the interlaced β-prism. The buried surface area in the helix bundle domain represents 31% of the total surface, and the head domain buried surface area is 1467 Å^2 for each monomer (average), which represents 29% of its whole surface (5138 Å^2).

The N-terminal Domain—The three-parallel helix bundle domain, encompassing residues 16/17–30 is assembled through side chain non-polar contacts as frequently observed in these structures (33). The missing 15/16 residues are also predicted to have a helical structure by PSIPRED (34). The deviations in the helix orientations are due to packing contacts that tilt the direction of each helix, when superimposed with those of the two other domains, by up to 4.5 Å.

This 30-residue domain is much smaller than its counterpart in phage p2 RBP, the shoulder, which comprises 141 amino acids and has a β-barrel original fold (Fig. 1*C*). However, in p2 RBP, the assembly of the three individual domains forming the shoulder trimer is mediated by three short parallel helices (residues 19–32) located close to the 3-fold axis, in a similar location as those of TP901-1 RBP (Fig. 1, *B* and *C*). This N-terminal domain resembles closely other helical domains observed in viral proteins. A well documented occurrence is the bacteriophage T4 fibritin, a segmented coiled-coil structure (33, 35). Another striking homology is observed with the spike protein of the

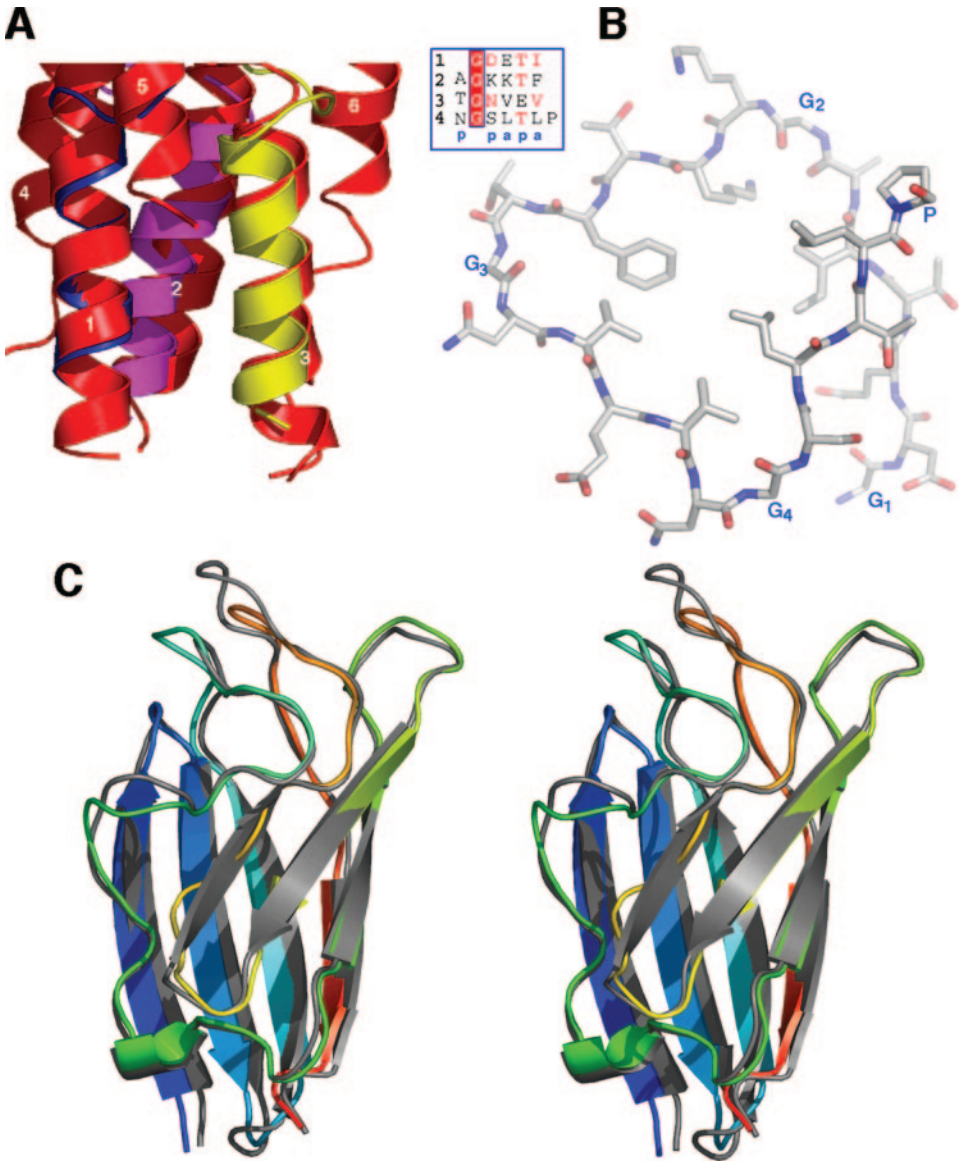

FIGURE 2. **Three-dimensional structure of lactococcal phages TP901-1 RBP domains.** *A*, the N-terminal three-helix bundle is colored *yellow*, *pink*, and *blue* (monomers A–C, respectively) and is superimposed on the three central helices of the SARS spike protein N terminus (six helices, in *red*). *B*, the neck β-helix isolated from a monomer; *inset*, the sequence repeat observed in this domain. *C*, stereo view of the head domain monomer of TP901-1 RBP, colored as a *rainbow* (*blue* to *red*), and superposed to the p2 RBP head domain (in *gray*). Note that a p2 RBP head β-strand is replaced by an elongated stretch (*yellow*) in TP901-1 RBP head.

SARS-associated coronavirus, formed of three central parallel helices surrounded by three external ones (36). The SARS spike central three-helix bundle superimposes well (r.m.s. deviation values of 0.9 Å for 10 Cα atoms) with the RBP N-terminal domain (Fig. 2*A*). This architecture of the parallel three-helix bundle is also observed frequently in other mammalian viral proteins involved in the fusion mechanism (37).

Following the helix bundle domain, a short linker structure (residues 31–39) connects the α-helical domain (residues 17–30) and the β-prism (residues 40–63) (Fig. 1*B*). A series of hydrogen bonds rigidifies this structure. Histidine 37 (*e.g.* from monomer B) plays a key role in this stabilization, since it binds both to residues from the helix bundle and residues from the β-prism. Its side chain atom N[cepsilon]2 is bound to the Glu^{28} main chain oxygen (2.8 Å), whereas its main chain nitrogen and oxygen are bound to Glu^{42} O[cepsilon]1 (2.82 Å) and His^{48C} Nζ, respectively.

The Neck—The β-prism neck domain interlaces three segments encompassing residues 40–63 of each subunit, organized into four β-strands (Figs. 1*B* and 2*B*). Each of the three faces of the prism is made of four β-strands from the three monomers constituting a parallel β-sheet. Such interlaced β-prisms have already been observed (reviewed by Mitraki *et al.* (33)) in the gp12 protein (short tail fibers) of coliphage T4 (32), in the RBP trimer of lactococcal phage p2 (16) and in a streptococcal lyase (38). The diameter of this β-prism is identical to that of gp12 of phage T4. Although similar to phage p2 neck, significant differences were observed (see "Discussion").

The neck sequence exhibits a six-amino acid, rather regular, repeating motif (Fig. 2*B*). This short motif is not observed either in gp12 or in the RBP neck of lactococcal phage p2. The first residue is a glycine, followed by a 2-fold repeat of two residues, a polar and a nonpolar. Each segment ends with a polar residue except the last one, where it is replaced by a proline. This proline, the last residue of the domain, redirects the peptidic chain to the top (as displayed in Fig. 1*B*), a feature already observed in the RBP neck of phage p2 (16).

The Recognition Head—The RBP head domain of TP901-1 (residues 64–163) (Fig. 1*B*) is a β-barrel formed of six antiparallel β-strands (Fig. 2*C*). It deviates from a double Greek key motif due to the presence of two nonregular extended structures that replace strands 4 and 7 (Fig. 2*C*). This domain is the only part of both RBPs (p2 and TP901-1) displaying sequence homology, displaying 28% sequence identity. Despite this low identity, both head domains exhibit very close structures (r.m.s. deviation values of 0.85 Å for the 114 Cα atoms in common between both monomers). Besides the presence of six regular β-strands instead of seven, the RBP head domain of TP901-1 deviates from that of p2 RBP

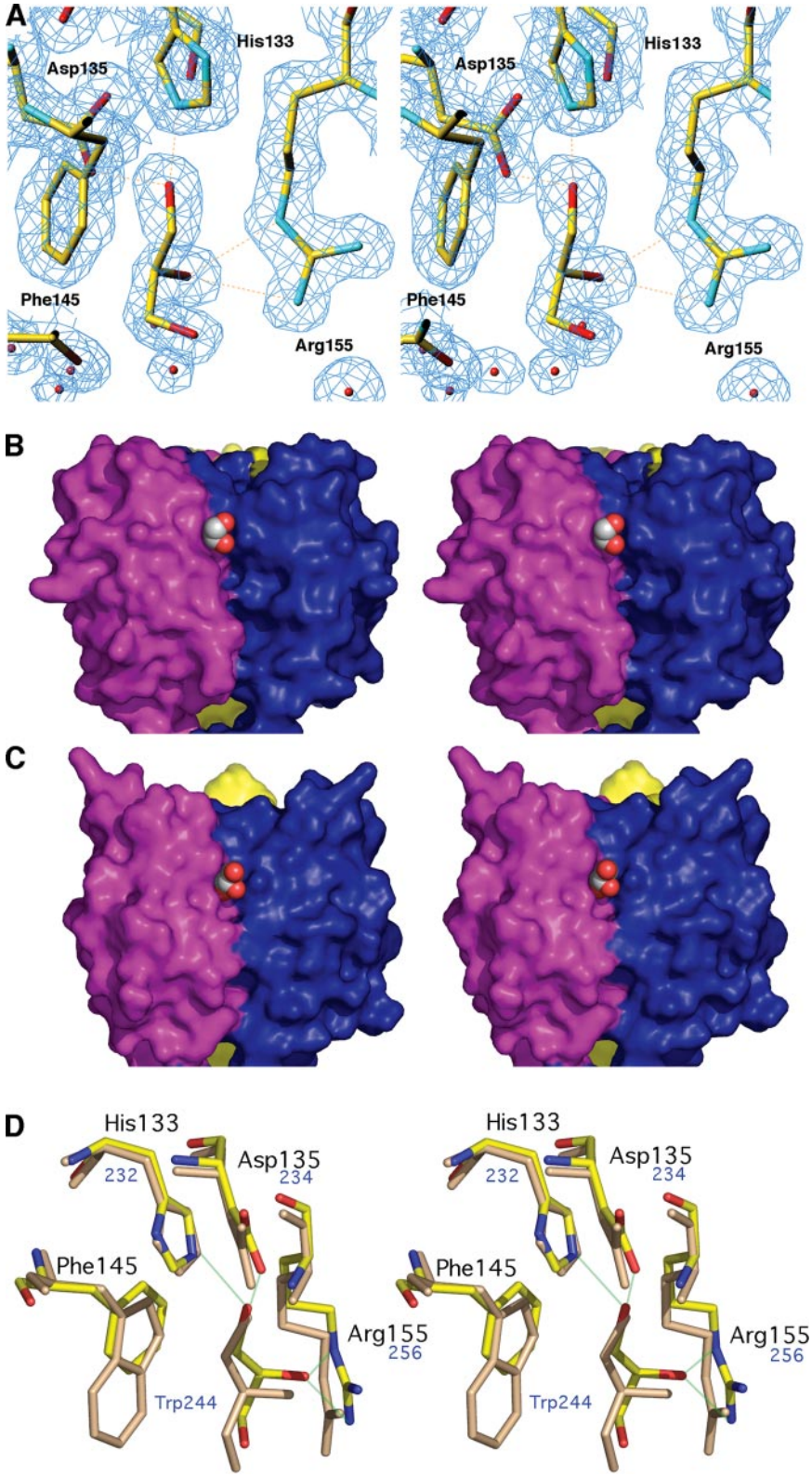

FIGURE 3. **Views of the glycerol-binding site in lactococcal phages TP901-1 RBP head.** *A*, stereo view of the electron density map (2fofc, 1σ) of the glycerol molecule (chain B) and its binding residues (view made with Turbo-Frodo (28)). *B*, stereo view of the molecular surfaces of glycerol in its binding site between monomers B and C of TP901-1 RBP head trimer; *C*, stereo view of the same portion of p2 RBP head trimer at the same scale with the same binding site. The monomers A–C are colored *yellow*, *pink*, and *blue*, respectively. Note the similar position and orientation of the glycerol molecule and the *crevice* prolonging the site above the glycerol. *D*, stereo view of the superposed structure of glycerol and its binding site in TP901-1 RBP head trimer and in p2 RBP head trimer, in *atom color code* or *pale rose*, respectively. The TP901-1 numbering is in *black*, and the p2 numbering is in *blue*. Views *B–D* were made with Pymol (available on the World Wide Web at www.pymol.org).

in a few loops (Fig. 2*C*). Contrary to p2, the RBP of phage TP901-1 has three cysteine residues in its sequence. Their sulfhydryl groups are free and not involved in disulfide bridging. The large distance between any pair formed between them forbids any speculation about the possibility of establishing a disulfide bridge.

The Putative Binding Site to the Host Receptor—A glycerol molecule was observed bound to the head domain. This molecule is better defined in monomer B, compared with monomers A or C. Their average B-factors reflect this fact, since their values are 29, 17, and 23 Å^2 in monomers A, B, and C, respectively. Glycerol molecules (Fig. 3, *A* and *D*) are stacked against Phe^{145} and establish hydrogen bonds with His^{133}, Asp^{135}, and Arg^{155}. As deduced from the sequence alignment of both RBPs (Fig. 1*A*), three of these residues are identical to those of phage p2 RBP, and the fourth, Phe^{145}, is a tryptophan (Trp^{244}) in p2 RBP. Two

hydroxyl groups from the glycerol molecule are therefore strongly bound to the RBP head. In contrast, the third hydroxyl group is free and points to the bulk solvent in both RBPs (Fig. 3, *B* and *C*). This orientation strongly suggests that the saccharidic binding site harbors the terminal residue of the receptor polymer, the free hydroxyl group pointing in the direction of the rest of the receptor polymer attached to the host.

The superposition of the binding network of glycerol in both RBPs is strikingly similar (Fig. 3*D*). Differences in amino acids are observed only in the second binding sphere, which modulate the binding crevice surface and volume and, hence, may influence the saccharidic specificity observed between different phage and bacterial strains (Table 2).

Tryptophan Fluorescence Quenching—Contrary to the case of p2 RBP (15), the lack of tryptophan as part of or in the vicinity of the glycerol-binding site prevented us from performing binding studies using tryptophan fluorescence quenching with glycerol or other saccharides.

An F145W mutant has therefore been generated, produced, and purified. Fluorescence quenching of tryptophan was performed with five saccharides: glycerol, phosphoglycerol, *N*-acetylmuramic acid, muramyl-dipeptide, and galactose. In the five cases, despite the presence of three other tryptophans, the signal at 340 nm was quenched. The four first sugars quenched ~20% of the signal, whereas galactose only quenched ~15% of it. This reflects also the affinity of these sugars for BppL (Table 3). The muramyl-dipeptide binds strongly to TP901-1 RBP, followed by *N*-acetylmuramic acid, glycerol, and phosphoglycerol and, last, by galactose.

Comparison with Electron Microscopy Data—Observation of the baseplate of phage TP901-1 with a transmission electron microscope revealed that TP901-1 baseplate is composed of two "disks," the upper and lower ones (19). The lower disk has been attributed to the assembly of several RBP (BppL) molecules. The lower disk appears as a series of spheres joining the upper disk through thin peduncles (Fig. 4*A*). Considering the average size of the baseplate as determined by transmission electron microscope (~200–220 Å), it is possible to identify six spheres (Fig. 4*B*) and to scale the RBP structure onto the electron microscopy view (Fig. 4*C*). The size of the head domain fits well with that of the bulbs, whereas the β-prism and the N-terminal domains might represent the peduncles (Fig. 4*C*).

DISCUSSION

This study provides further evidence that the nature of the host receptor of lactococcal phages is saccharidic. The fact that glycerol tightly binds to the RBP of phage p2 (15) strongly suggested that the host receptor molecule might be a (lipo)teichoic acid polymer. Glycerol or phosphoglycerol also bind tightly to the RBP of phage TP901-1, but less than the muramyl dipeptide (Table 3). It cannot be excluded, therefore, than muramyl dipeptide might be part of the host receptor. However, teichoic or lipoteichoic acids are more prone to ensure strain specificity. They consist of a saccharidic polymer pointing out of the cell wall with a chain of substituted polyglycerol phosphate (39). The central hydroxyl group is either free or substituted by a D-glucose or a D-alanine, a feature that might be involved in strain specificity. Interestingly, despite the different strains of *L. lactis* recognized by p2 and TP901-1 phages (*L. lactis* strains LM0230 and 3107, respectively), their glycerol binding sites are very similar (this study) (15). This suggests that secondary sites might be involved in the whole polysaccharide recognition or that the different decorations of the first phosphoglycerol moiety might both modulate the strain recognition and increase the affinity for TP901-1 RBP.

The RBP structure of the temperate lactococcal phage TP901-1, a member of the P335 species, exhibits a modular assembly, in a similar fashion as that observed in the RBP of the lytic lactococcal p2 phage of the 936 species (16). The head receptor recognition modules are similar in both phages (28% identity). We have shown previously that the head domain of phage p2 RBP has a fold similar to that of RBPs of mammalian viruses (16), reovirus (30), and adenovirus (31). This observation extends now to another genetically distinct phage of the *Siphoviridae* family. In contrast, the shoulder domains anchoring the RBP in the phage baseplate are totally different between p2 and TP90-1. The neck domain, which links the shoulders and the head domains, is superficially similar in both molecules, presenting an interlaced β-prism fold. However, both prisms differ in their number of residues per turn, 17 and 19 for the RBPs of p2 and TP901-1, respectively. Hence, the RBP prism of TP901-1 has a larger radius compared with that of p2. Furthermore, phage TP901-1 RBP neck exhibits a six-residue repeat, which is not the case for the RBP neck of phage p2.

Recently, the genes responsible for host recognition in the lactococcal virulent phages bIL170 and sk1 (a close relative of p2) belonging to species 936 were also identified (11). These phages have a high level of DNA identity but different host ranges. Functional chimeric bIL170 phages carrying RBP gene from sk1 were generated, and the recombinant phages were able to only infect the host of phage sk1. The comparison of the RBPs of phages p2/sk1 with that of bIL170 revealed a striking difference in the identity of the modules. The N-terminal shoulder domains of both phages are quasi-identical, whereas the neck and the head domains do not exhibit any sequence similarity. The shoulders being probably the modules in contact with other proteins of the phage baseplate, their strong similarity made it possible (8) to exchange the RBPs between both phages and switch their specificity. If the shoulders had been different, the experiment would have led to nonfunctional phages.

A similar RBP swapping experiment was recently performed with phages belonging to the P335 species. Temperate phages TP901-1 and tuc2009 share a large genomic similarity, specifically in the genes coding for proteins involved in phage morphogenesis (20). Their RBPs, however, exhibit the same modular differences as those observed between sk1 and bIL170 of the 936 species. The N-terminal sequences (residues 1–60) are highly similar, whereas the head domain sequences exhibit no similarity and possibly possess different folds. Therefore, a common conserved motif of the three-parallel helix bundle (as revealed by the structure solved here and secondary structure prediction) seems to anchor the RBP to the phage baseplate (most probably ORF48 (19)),

TABLE 2
Second shell residue comparison between TP901-1 and p2 RBPs

TP901-1 BppL	p2 RBP
Val^{126B}	Ala^{225B}
Thr^{153B}	Ala^{254B}
Gly^{91B}	Phe^{191B}
Arg^{118B}	Val^{217B}
Gln^{143A}	Thr^{242A}

TABLE 3
***K_d* constants (in nM) of several saccharides for TP901-1 BppL (this work) and p2 RBP or p2 RBP head domain (15)**

	Glycerol	Glycerol phosphate	Galactose	*N*-acetylmuramic acid	*N*-acetylmuramic dipeptide
BppL TP901-1 F145W	50 ± 5	50 ± 7	1400 ± 200	30 ± 4	4 ± 0.4
RBP p2 (15)	260 ± 50	130 ± 30	170 ± 30	NA[a]	120 ± 30
RBP p2 head (15)	180 ± 40	120 ± 30	160 ± 30	NA	140 ± 30

[a] NA, not available.

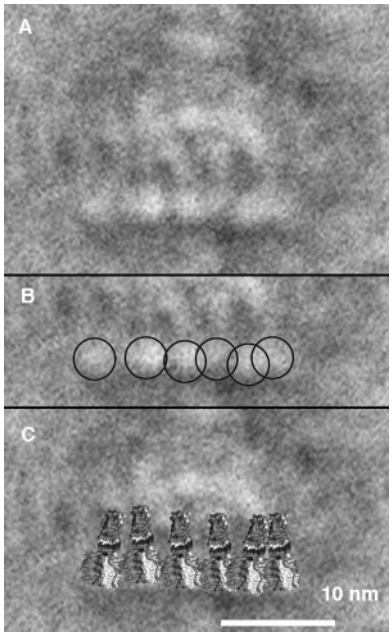

FIGURE 4. **Modeling of TP901-1 RBP onto the electronic microscopy picture of the phage.** *A*, the EM view of the baseplate alone (EM image provided by Christina S. Vegge and Horst Neve) (12, 20). *B*, same picture, with the lower baseplate bulbs identified with *black circles*. *C*, *ribbon views* of the RBP structure adjusted to the scale of the EM picture and superimposed onto the bulbs of the lower baseplate.

whereas the receptor recognition domains differ highly, in agreement with their distinct host range. The structural closeness of the phage anchoring domain in phages TP901-1 and tuc2009 again made it possible to swap the RBPs and the host specificity. Amazingly, the head recognition domains of the p2 and TP901-1 RBPs, while belonging to two different lactococcal phage species, are closer in sequence (and probably in structure) than RBPs from phages of the same species (p2/sk1 *versus* bIL170 and TP901-1 *versus* tuc2009). Experiments are under way to validate this hypothesis.

CONCLUSION

Phages are subject to a double constraint. They must maintain the cohesion of the proteins involved in virion assembly and replication (40) as well as modify at a relatively fast pace the proteins involved in host recognition in order to follow the genetic drift of their host or to reach new host strains. Lactococcal phages seem to fulfill this double constraint by gathering three subsets of structural repertoires in their RBPs. The N-terminal domain is part of the phage core and makes it possible to anchor the RBP to the rest of the phage baseplate. It is conserved between phages that are genetically close. A short and rigid neck domain serves to link the phage anchored domain and the head. Following the neck, the head domain is involved in the fine tuned recognition of one of the many receptor structures of the different *L. lactis* host strains. Although the head domain seems to share a common saccharide-binding motif, the variation of a few residues of the second binding sphere may be involved in this fine tuning.

Acknowledgments—We thank Lone Brøndsted, Finn Vogensen, and Denise Tremblay for helpful discussions, and we thank Christina S. Vegge and Horst Neve for providing EM pictures of phage TP901-1.

REFERENCES

1. Moineau, S., Tremblay, D., and Labrie, S. (2002) *ASM News* **68**, 388–393
2. Moineau, S., Fortier, J., and Ackermann, H.-W. (1992) *Can. J. Microbiol.* **38,** 875–882
3. Moineau, S. M., Borkaev, B. J., Holler, S. A., Walker, J. K., Kondo, E. R., Vedamuthu, and Vandenbergh, P. A. (1996) *J. Dairy Sci.* **79**, 2104–2111
4. Bissonnette, F., Labrie, S., Deveau, H., Lamoureux, M., and Moineau, S. (2000) *J. Dairy Sci.* **83,** 620–627
5. Josephsen, J., and Nielsen, E. W. (1988) *Milchwissenschaft* **43,** 219–223
6. Josephsen, J., and Neve, H. (1998) in *Lactic Acid Bacteria: Microbiology and Functional Aspects* (Salminen, S., and von Wright, A., eds) pp. 385–436, Marcel Dekker, Inc., New York
7. Moineau, S., Pandian, S., and Klaenhammer, T. R. (1993) *Appl. Environ. Microbiol.* **59,** 197–202
8. Dupont, K., Vogensen, F. K., Neve, H., Bresciani, J., and Josephsen, J. (2004) *Appl. Environ. Microbiol.* **70,** 5818–5824
9. De Haard, H. J., Bezemer, S., Ledeboer, A. M., Muller, W. H., Boender, P. J., Moineau, S., Coppelmans, M. C., Verkleij, A. J., Frenken, L. G., and Verrips, C. T. (2005) *J. Bacteriol.* **187,** 4531–4541
10. Deveau, H., Van Calsteren, M. R., and Moineau, S. (2002) *Appl. Environ. Microbiol.* **68,** 4364–4369
11. Dupont, K., Janzen, T., Vogensen, F. K., Josephsen, J., and Stuer-Lauridsen, B. (2004) *Appl. Environ. Microbiol.* **70,** 5825–5832
12. Geller, B. L., Ngo, H. T., Mooney, D. T., Su, P., and Dunn, N. (2005) *J. Dairy Sci.* **88,** 900–907
13. Valyasevi, R., Sandine, W. E., and Geller, B. L. (1990) *Appl. Environ. Microbiol.* **56,** 1882–1889
14. Valyasevi, R., Sandine, W. E., and Geller, B. L. (1994) *J. Dairy Sci.* **77,** 1–6
15. Tremblay, D. M., Tegoni, M., Spinelli, S., Campanacci, V., Blangy, S., Huyghe, C., Desmyter, A., Labrie, S., Moineau, S., and Cambillau, C. (2006) *J. Bacteriol.* **188,** 2400–2410
16. Spinelli, S., Desmyter, A., Verrips, C. T., de Haard, H. J., Moineau, S., and Cambillau, C. (2006) *Nat. Struct. Mol. Biol.* **13,** 85–89
17. Ledeboer, A. M., Bezemer, S., de Hiaard, J. J., Schaffers, I. M., Verrips, C. T., van Vliet, C., Dusterhoft, E. M., Zoon, P., Moineau, S., and Frenken, L. G. (2002) *J. Dairy Sci.* **85,** 1376–1382
18. Brondsted, L., Ostergaard, S., Pedersen, M., Hammer, K., and Vogensen, F. K. (2001) *Virology* **283,** 93–109
19. Vegge, C. S., Brondsted, L., Neve, H., McGrath, S., van Sinderen, D., and Vogensen, F. K. (2005) *J. Bacteriol.* **187,** 4187–4197
20. Vegge, C. S., Vogensen, F. K., Mc Grath, S., Neve, H., van Sinderen, D., and Brondsted, L. (2006) *J. Bacteriol.* **188,** 55–63
21. Walhout, A. J., Temple, G. F., Brasch, M. A., Hartley, J. L., Lorson, M. A., van den Heuvel, S., and Vidal, M. (2000) *Methods Enzymol.* **328,** 575–592
22. Sulzenbacher, G., Gruez, A., Roig-Zamboni, V., Spinelli, S., Valencia, C., Pagot, F., Vincentelli, R., Bignon, C., Salomoni, A., Grisel, S., Maurin, D., Huyghe, C., Johansson, K., Grassick, A., Roussel, A., Bourne, Y., Perrier, S., Miallau, L., Cantau, P., Blanc, E., Genevois, M., Grossi, A., Zenatti, A., Campanacci, V., and Cambillau, C. (2002) *Acta Crystallogr. Sect. D Biol. Crystallogr.* **58,** 2109–2115
23. Matthews, B. W. (1968) *J. Mol. Biol.* **33,** 491–497
24. Zheng, L., Baumann, U., and Reymond, J. L. (2004) *Nucleic Acids Res.* **32,** e115
25. Collaborative Computing Project 4 (1994) *Acta Crystallogr. Sect. D* **50,** 760–766
26. Navaza, J. (1994) *Acta Crystallog. Sect. A* **50,** 157–163
27. Murshudov, G., Vagin, A. A., and Dodson, E. J. (1997) *Acta Crystallogr. Sect. D* **53,** 240–255
28. Roussel, A., and Cambillau, C. (1991) *The TURBO-FRODO Graphics Package*, Silicon Graphics, Mountain View, CA
29. Laskowski, R., MacArthur, M., Moss, D., and Thornton, J. (1993) *J. Appl. Crystallogr.* **26,** 91–97
30. Chappell, J. D., Prota, A. E., Dermody, T. S., and Stehle, T. (2002) *EMBO J.* **21,** 1–11
31. Burmeister, W. P., Guilligay, D., Cusack, S., Wadell, G., and Arnberg, N. (2004) *J. Virol.* **78,** 7727–7736
32. van Raaij, M. J., Schoehn, G., Burda, M. R., and Miller, S. (2001) *J. Mol. Biol.* **314,** 1137–1146
33. Mitraki, A., Miller, S., and van Raaij, M. J. (2002) *J. Struct. Biol.* **137,** 236–247
34. McGuffin, L. J., Bryson, K., and Jones, D. T. (2000) *Bioinformatics* **16,** 404–405
35. Tao, Y., Strelkov, S. V., Mesyanzhinov, V. V., and Rossmann, M. G. (1997) *Structure* **5,** 789–798
36. Xu, Y., Lou, Z., Liu, Y., Pang, H., Tien, P., Gao, G. F., and Rao, Z. (2004) *J. Biol. Chem.* **279,** 49414–49419
37. Schibli, D. J., and Weissenhorn, W. (2004) *Mol. Membr. Biol.* **21,** 361–371
38. Smith, N. L., Taylor, E. J., Lindsay, A. M., Charnock, S. J., Turkenburg, J. P., Dodson, E. J., Davies, G. J., and Black, G. W. (2005) *Proc. Natl. Acad. Sci. U. S. A.* **102,** 17652–17657
39. Delcour, J., Ferain, T., Deghorain, M., Palumbo, E., and Hols, P. (1999) *Antonie Leeuwenhoek* **76,** 159–184
40. Bamford, D. H., Burnett, R. M., and Stuart, D. I. (2002) *Theor. Popul. Biol.* **61**, 461–470

Modular Structure of the Receptor Binding Proteins of *Lactococcus lactis* Phages: THE RBP STRUCTURE OF THE TEMPERATE PHAGE TP901-1

Silvia Spinelli, Valérie Campanacci, Stéphanie Blangy, Sylvain Moineau, Mariella Tegoni and Christian Cambillau

J. Biol. Chem. 2006, 281:14256-14262.
doi: 10.1074/jbc.M600666200 originally published online March 20, 2006
